Title

Computational Evaluation of Venous Graft Geometries in Coronary Artery Bypass Surgery

Journal

Seminars in Thoracic and Cardiovascular Surgery, 34(2)

ISSN

1043-0679

Authors

Seo, Jongmin
Ramachandra, Abhay B
Boyd, Jack
et al.

Publication Date

2022

DOI

10.1053/j.semtcvs.2021.03.007

Peer reviewed

HHS Public Access

Author manuscript

Semin Thorac Cardiovasc Surg. Author manuscript; available in PMC 2023 July 01.

Published in final edited form as:

Semin Thorac Cardiovasc Surg. 2022 ; 34(2): 521–532. doi:10.1053/j.semtcvs.2021.03.007.

Computational evaluation of venous graft geometries in coronary artery bypass surgery

Jongmin Seo, PhD[a,b,†], **Abhay B. Ramachandra, PhD**[c,†], **Jack Boyd, PhD, MD**[d], **Alison L. Marsden, PhD**[a,b], **Andrew M. Kahn, PhD, MD**[e]

[a]Departments of Pediatrics (Cardiology), and Stanford University, Stanford, CA

[b]Departments of Bioengineering, and Stanford University, Stanford, CA

[c]Department of Biomedical Engineering, Yale University, New Haven, CT,

[d]Departments of Cardiothoracic Surgery, and Stanford University, Stanford, CA

[e]Division of Cardiovascular Medicine, University of California San Diego, La Jolla, CA.

Abstract

Objectives: Cardiothoracic surgeons are faced with a choice of different revascularization techniques and diameters for saphenous vein grafts (SVG) in coronary artery bypass graft surgery (CABG). Using computational simulations, we virtually investigate the effect of SVG geometry on hemodynamics of both venous grafts and the target coronary arteries.

Methods: We generated patient-specific three-dimensional anatomic models of CABG patients and quantified mechanical stimuli. We performed virtual surgery on three patient-specific models by modifying the geometry vein grafts to reflect single, Y, and sequential surgical configurations with SVG diameters ranging from 2 mm to 5 mm.

Corresponding author: Andrew Kahn, Ph.D., M.D. Professor, University of California, San Diego, School of Medicine, Division of Cardiovascular Medicine, 200 W. Arbor Drive #8411, San Diego, CA 92103 858.657.5378 (office phone) akahn@ucsd.edu.
[†]These authors contributed equally to this work.

Disclosures: Two of the authors (A.L.M. and A.M.K. are co-inventors of a patent that is broadly related to this work). The authors have nothing to disclose with regard to commercial support and no other potential conflicts.

Abbreviated legend for Central Picture:
Patient-specific vascular model coupled with circuit model of chambers and circulations.

Central Message
The coronary runoffs are insensitive to the choice of the saphenous vein graft geometry. Wall shear stress can be a valuable guiding metric in the choice of revascularization geometries.

Abbreviated Legend for the Central Picture
Computational evaluation of venous graft geometries in coronary artery bypass surgery.

Perspective Statement
Using computational simulation we virtually investigate the effect of vein graft geometry on hemodynamics of grafts and target coronary arteries. Coronary artery runoffs are insensitive to vein graft geometry. Wall shear stress of grafts increases non-linearly with decreasing diameter following an inverse power scaling, and can be a valuable guiding metric in the choice of revascularization geometries.

Results: Our study demonstrates that the coronary artery runoffs are relatively insensitive to the choice of SVG revascularization geometry. We observe a 10% increase in runoff when the SVG diameter is changed from 2 mm to 5 mm. The wall shear stress (WSS) of SVG increases dramatically when the diameter drops, following an inverse power scaling with diameter. For a fixed diameter, the average wall shear stress on the vein graft varies in ascending order as single, Y, and sequential graft in the patient cohort.

Conclusions: The runoff to the target coronary arteries changes marginally due to the choice of graft configuration or diameter. The shear stress on the vein graft depends on both flow rate and diameter and follows an inverse power scaling consistent with a Poiseuille flow assumption. Given the similarity in runoff with different surgical configurations, choices of SVG geometries can be informed by propensity for graft failure using shear stress evaluations.

Graphical Abstract

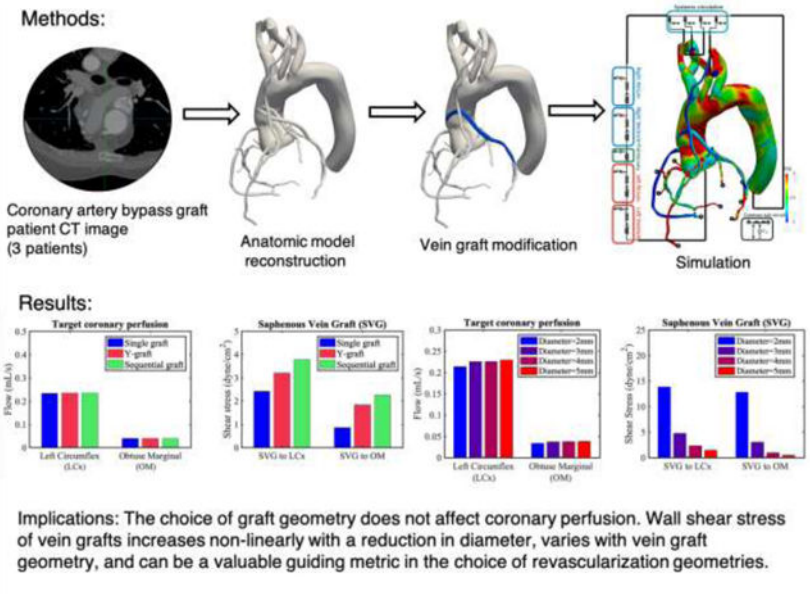

Keywords

Coronary artery bypass graft surgery (CABG); blood flow simulation; virtual surgery; vein graft; shear stress

INTRODUCTION

Coronary artery bypass graft surgery (CABG) with vein grafts is the mainstay of multivessel surgical revascularization in coronary artery disease due to limited availability of arterial grafts. In multi-target revascularization, cardiothoracic surgeons are often faced with choices of different revascularization geometries and sizes for saphenous venous grafts (SVG). Decisions regarding preferable vein graft configurations rely on retrospective studies, surgeons' intuition, training, and experience, as well as the available saphenous veins. Prior studies comparing the efficacy and superiority of revascularization techniques between single and sequential grafts show mixed results. Some studies report superior patency of

sequential configurations over single configurations [1,2,3], others report no significant difference in the myocardial infraction, mortality rate, reintervention, between the single and sequential vein grafts [1,4], and yet others show worse patency of sequential vein grafts compared to single vein grafts [5,6]. Additional studies report comparable graft patency between Y-grafts and sequential grafts [7,8]. Further, the choice of SVG diameter, which can vary in different segments of the SVG, can affect outcomes of these techniques. While diameter of the saphenous vein graft has been identified as one of the key factors affecting the vein graft patency in CABG [9,10], there is currently no quantitative comparison of the performance of these surgical methodologies, especially under varying diameters and controlled conditions.

It is well known that hemodynamics, wall mechanics, and geometry play a critical role in the long-term adaptation of vein grafts [9,10,11]. Specifically, low wall shear stress (WSS) and high oscillatory wall shear index (OSI) has been identified as an important mechanical stimulus for atherosclerosis progression in arteries [12]. Although the pathophysiology of vein graft failure may be different from arteries, animal studies [13,14] have shown strong correlation between low wall shear stress and intimal hyperplasia in vein grafts. Image-based cardiovascular simulations using computational fluid dynamics (CFD) techniques provide a non-invasive means to quantify mechanical stimuli on vein grafts in patient-specific geometries [15,16,17]. A few studies [18,19] have applied virtual surgeries in cardiovascular models to evaluate the different revascularization methodologies in CABG surgery albeit these studies relied on reduced order or idealized models with limited patient-specific data. In this study, we performed simulations on patient-specific cardiovascular CABG models to quantitatively compare several revascularization geometries commonly used in clinical practice, while systematically varying the size of the implanted vein grafts. We use CT images of patients who had undergone CABG surgeries to build our models. Hemodynamic quantities of mechanobiological relevance such as pressure, flow, wall shear stress, and oscillatory shear index are quantified from simulation data.

MATERIALS AND METHODS

Clinical Data Acquisition

Patient recruitment and access to non-invasive clinical data was carried out according to protocols approved by the Stanford University and University of California San Diego Institutional Review Boards. Informed consent was obtained from all patients included in the study.

Image Acquisition

Patients were scanned using a 64-slice Discovery CT750 HD scanner (GE Healthcare, Chicago, IL). Oral and/or intravenous metoprolol was administered as needed to decrease the patients' heart rate, with a goal heart rate of 60 beats/min, and 0.4 mg of sublingual nitroglycerin was given prior to the scan. Iodinated contrast was injected with a triple-phase technique (contrast, contrast/saline mix, and saline) with the dose, mixture, and flow rate adjusted for the patients' BMI. Images were obtained during a single breath-hold using

padded prospective gating with imaging centered at 75% of the R-R interval and a slice thickness of 0.625 mm.

Patient characteristics

Patient demographic information is summarized in Table 1. One patient received a Y-graft geometry and two patient received sequential graft geometries. The Y-graft in Patient 1 is connected to the diagonal branch of left coronary artery (DIAG) and the posterior descending artery (PDA). The sequential graft in Patient 2 is proximally anastomosed to the Ramus and distally anastomosed to obtuse marginal (OM). The sequential graft in Patient 3 is proximally anastomosed to OM and distally anastomosed to left circumflex artery (LCx). Other SVGs and internal mammary arteries are single anastomosis grafts.

Model Construction and Simulation

Modeling and simulation were performed using the open source software SimVascular (www.simvascular.org) [20]. Patient-specific 3D models of CABG geometries were built from CT images of the three patients who had previously undergone bypass surgery (Table 1). The models were discretized using linear tetrahedral finite elements using MeshSim software (Simmetrix Inc, Troy, NY). Convergence of flow, pressure, and wall shear stress distributions within 10% error were confirmed with multiple successive mesh adaptation and refinements. Each patient model had approximately 3.5–4.5M tetrahedral elements after mesh adaptation.

We used lumped parameter networks (LPN) as boundary conditions to the 3-D patient-specific models to mimic the pressure-flow relationships in the systemic circulation, coronary circulation and the heart [15,22] (Figure E1). The LPNs were tuned for each patient to match routinely collected non-invasive clinical data, including cuff blood pressure, stroke volume, cardiac output as measured by echocardiography, and empirical data from literature for the percentage of cardiac output perfusing the coronaries [16] (Table E1). We employed fluid-structure interaction using the coupled momentum method [22] and assigned vessel specific material properties (0.7 MPa for the aorta and the arch walls, 1.4 MPa for internal mammary arteries, 1.15 MPa for coronary arteries, 5 MPa for vein grafts), and thickness for coronary arteries and bypass grafts [23] based on literature, as in our previous work [16]. The vessels are modeled to be linearly elastic.

To isolate the effect of varying surgical geometry, we first built a model based on the CT data with the original surgical configuration for each patient (Table 1). With guidance from surgeons, we virtually modified the venous grafts to simulate three revascularization techniques: single, Y, and sequential graft configurations. Simulations were run for each surgical configuration keeping rest of the simulation parameters, including boundary conditions, material properties, and remaining anatomy, fixed. Figure 1 summarizes the computational models for three CABG patients with anatomic variations for the three surgical configurations.

Further, to elicit the effect of graft diameter on hemodynamics and distal perfusion, we changed the diameter of the single SVGs in each patient model. We extracted the centerline

of each vein graft and then calculated the equivalent diameter of the vein, $d_{eqv}(x) = \sqrt{\frac{A(x)}{\pi/4}}$ (millimeters), where $A(x)$ is the cross-sectional area (mm^2) of the vessel at location x along the centerline. We spatially averaged equivalent diameter for the entire graft to report an averaged diameter of SVG, D_{SVG} (Table E2). The virtual patient models were generated with scaled segmentations of the SVG, in which the original distances from the centerline were multiplied by the shape factor $\frac{D_{modified}}{D_{original}}$ where $D_{modified}$ and $D_{original}$ are the averaged diameter of each SVG in the scaled and original model, respectively. Since the scaled cross sections were centered on the same centerline, the curvature of the graft was maintained. Ten virtual patient models with single SVGs were generated with diameters of 2 mm, 3 mm, 4 mm, and 5 mm (Figure E2); the range of diameters were informed by literature and our surgical colleagues [9,10,16,23,24].

Cardiovascular simulations were performed in parallel on 96 CPU cores for each simulation using the Comet supercomputing cluster available through the Extreme Science and Engineering Discovery Environment. We report results from the 6^{th} cardiac cycle, after the numerical transients have disappeared and results reached a cyclic periodicity.

Postprocessing

In addition to pressure and flow to the target coronaries, we quantify key mechanobiological stimulus, time averaged wall shear stress (TAWSS) and oscillatory shear index (OSI), which influences endothelial behavior and is implicated in early intimal hyperplasia, and cell proliferation. We also report WSS_{avg}, which is the spatially averaged TAWSS over the length of the SVG segment (Table E2).

In the sequential graft, WSS_{avg} is individually obtained in the proximal and distal region after anastomosis, whereas in the Y graft, WSS_{avg} is calculated in the main vessel connecting the distal coronary target and also include the trunk of Y, and the branch off the main vessel connecting to the proximal target coronary.

We propose two metrics of probable clinical utility, $WSS_{Poiseuille}$ and R_{SVG}, derived from the analytical solution of Poiseuille flows. We estimated the wall shear stress, under the assumptions of a steady, laminar flow in a circular cylinder,

$$WSS_{Poiseuille}(x) = \frac{32\mu Q}{\pi d_{eqv}(x)^3}\left(\frac{dyne}{cm^2}\right), \quad (1)$$

where the μ (dyne · sec/cm^2) is dynamic viscosity of blood, Q (cm^3/sec) is the blood flow rate obtained from the simulation data.

The vascular resistance of the SVG under the Poiseuille flow assumption is,

$$R_{SVG} = \frac{8\mu L_{SVG}}{\pi D_{SVG}^4}\left(dyne \cdot \frac{sec}{cm^5}\right), \quad (2)$$

can be used as a measure of viscous shear in the venous grafts [27] where L_{SVG} and D_{SVG} is the length and diameter of SVG respectively. R_{SVG} can be used as a measure of viscous resistance in the venous grafts [27].

RESULTS

Quantification of hemodynamics in virtually revascularized geometries

Single, Y, and sequential configurations have comparable distal runoffs suggesting that the choice of revascularization geometry does not affect acute perfusion, as distal demand and the associated vascular resistance dominates the runoff to the target coronary (Figure 2 a,d,g). Compared to single, Y grafts consistently have higher WSS_{avg} across patients when the proximal region is included in the comparison (Figure 2 c,f,i). All oscillatory shear index (OSI) values were below 0.1 and we found no observable difference in OSI among the three different revascularization methodologies (data not shown).

The effect of surgical revascularization geometries on spatial variation of TAWSS along the graft is summarized in Figure 3. Note that, due to mass conservation, the flow in a given graft is constant until it reaches an anastomotic site (Figure 3 a,e,i). Despite sections of constant flow one can observe variation in TAWSS along the length of the graft, attributable to local variations in diameter. Figure 3 demonstrates the interplay between flow and graft diameter and its effect on cross-sectional TAWSS. In sequential grafts, the reduced flow (0.46 to 0.25 mL/sec in Patient 2, and 0.42 to 0.34 mL/sec in Patient 3) after anastomosis is compensated by the tapered vessel diameter from the proximal to distal region ($D_{SVG,\ proximal}$ = 4.8 mm to $D_{SVG,\ distal}$ = 3.6 mm in Patient 2, and $D_{SVG,\ proximal}$ = 4.5 mm to $D_{SVG,\ distal}$ = 3.8 mm in Patient 3). The consistently higher WSS_{avg} in Y grafts compared with the single grafts (Figure 2) is associated with the higher TAWSS in the trunk of the Y grafts. While these results demonstrate the utility of CFD in virtual surgical comparison and hemodynamic quantification, the interplay between distal demand and graft dimension makes it hard to discern a trend in these vascular geometries. Therefore, we controlled for diameter alone in the next section.

Effects of vein graft diameter

Increasing the SVG diameter increased flow and pressure in the target coronaries marginally (Figure 4) in the single graft configuration. A change in diameter from 2 mm to 5 mm increased the flow to the target coronary by approximately 7 to 10 % (Figure 4 a,e,h). Although vascular resistance of the SVG changes 39 fold for a change in diameter from 5 mm to 2 mm, the native coronary artery resistance is much larger, consistent with results in Table 1, and therefore dominates flow through the grafts.

We observed large variabilities in wall shear stress with changing SVG diameter (Figure 4). WSS_{avg} is noticeably high ($\geqslant$ 14 dyne/cm^2) when D_{SVG} = 2 mm. WSS_{avg} drops below 10 dyne/cm^2 when SVG diameter is larger than 3 mm and is very low ($\leqslant$ 1.5 dyne/cm^2) when D_{SVG} = 5 mm in a single graft configuration.

In Figure 5, the TAWSS distributions obtained from CFD are plotted against TAWSS obtained from Poiseuille flow assumptions. We investigated the scaling relationship between

WSS_{avg} and D_{svg} by using the linear regression on data in Figure 5(b) using the relationship $\log(WSS_{avg}) = m^*\log(D_{svg}) + n$. We obtained $WSS_{avg} \sim D_{svg}^{-3.01 \pm 0.34}$, by taking average of the regression coefficients for six grafts, all showed $R^2>0.99$ for their linear regressions. Although $WSS_{Poiseuille}$ underestimates the WSS estimate on the vein grafts from CFD, the trend of TAWSS with the varying diameter was well-captured by the scaling relationship of $WSS_{Poiseuille} \sim \frac{1}{D^3}$ in equation (1) and makes it a potential inexpensive surrogate for an expensive 3D-CFD simulation. The inverse power relation also attributes the low WSS_{avg} in single grafts, compared to sequential and Y-graft, to the larger cross-sectional area. The inverse power relationship motivated us to further probe its utility in a clinical decision-making process.

To show the utility of the inverse power scaling relation and quantify the effect of diameter on surgical geometry, we evaluated TAWSS in all the three virtually created surgical configurations with D_{SVG} = 2 mm, 3 mm, 4 mm. In Figure 6, we recompute the TAWSS from flow values in Figure 2 with the inverse scaling law; we superimpose a line at 25 dyne/cm^2 to act as a reference for average WSS in the coronary circulation. Wide heterogeneity in TAWSS variation along the length is observed across patients, surgical configurations and graft diameter. For example, the proximal section of the sequential in Patient 1 has high TAWSS ($\geqslant$100 dyne/cm^2) for D_{SVG} = 2 mm which might make the proximal section prone to endothelial damage. By contrast, Y and single configurations in Patient 3 have sections of the graft with low TAWSS ($\leqslant$ 2 dyne/cm^2) at D_{SVG} = 3 mm and 4 mm, which might make them atheroprone. For a fixed diameter, across patients, TAWSS increases from single, Y, to sequential configuration, respectively (Figure 6) in the patient cohort.

DISCUSSION

Our study reveals several important findings. First, we demonstrate that the choice of vascular graft configuration does not lead to changes in perfusion to the target coronary artery. Flow through a vein graft primarily depends on the distal coronary resistance (more than 93% of the total resistance) rather than the vascular resistance of the graft itself (less than 6% of the total resistance). Second, it demonstrates that WSS acting on the vein graft shows large variabilities with surgical geometry and depends, not surprisingly, on both flow and graft diameter. Third, it confirms that the Poiseuille flow assumption is a good surrogate for the WSS computed in full 3D simulations. Fourth, it illustrates the potential clinical utility of the inverse power relationship, under Poiseuille flow assumptions, in the clinical decision-making process of choosing graft geometries and coronary targets. In this pilot study we do not claim the universal superiority of a vein graft configuration against another, but rather emphasize the importance of taking a patient-specific approach and suggest use of wall shear stress as a guiding metric in decision making process, as we observe that hemodynamics varies among patients and coronary targets in non-uniform ways.

The findings in this manuscript are consistent with findings in the literature. A recent finding by Li et al. [28] measured identical runoff from single and sequential graft configurations during the off-pump CABG surgery. Our results are also consistent with O' Neil et al. [24],

who demonstrated that coronary vascular resistance was a more important determinant of flow through the graft since the vein graft resistance was quite small compared to the distal coronary resistance.

Notwithstanding the deviations of WSS from CFD and Poiseuille calculations (Figure 5), we submit that the change of WSS largely follows the inverse power scaling of diameter and therefore serves as a valuable guiding metric. The inverse scaling of flow with diameter is well-established in cardiovascular flows, albeit with different power dependence across parts of circulation [27,29]. We do however note that the Poiseuille solution only provides understanding of the scaling relationship and an inexpensive, quick surrogate metric for decision making process, but cannot replace or predict the full spatial heterogeneity and distribution of WSS.

The influence of wall shear stress and diameter on vein graft patency has been previously acknowledged [30]. The 1-year follow up CABG study by [31] reported strong correlations between low wall shear stress, measured by the transit time flow measurement and solutions of the Poiseuille flow at the time of surgery, and decrease in graft diameter. The CASCADE clinical trial, in which 322 grafts were assessed [25], identified strong correlations between vein graft hyperplasia and SVG diameter, and hypothesized that larger grafts have lower shear stress and as a result, less hyperplasia. High wall shear stress and low wall shear stress have both been implicated in inducing a pathological response in endothelial cells. While low WSS has been shown to be atheroprone [13,14], high WSS is known to induce endothelial damage [32]. In a recent retrospective study [17], low wall shear stress, when normalized by WSS obtained from Poiseuille flow assumption, was significantly associated with the SVG stenosis.

Despite the uncertainty in TAWSS conditions associated with improved graft patency, we can make observations regarding the effect of surgical geometry on TAWSS for the three patients in our study. The average wall shear stress on the vein graft increases from single, to Y, to sequential grafts for a fixed diameter (Figure 6). Locally, TAWSS varies along the length of the graft, and between patients. One would likely avoid sequential grafting in Patient 1 with D_{SVG} = 2 mm as the TAWSS is very high, whereas the sequential graft with 2 mm diameter could be preferred in Patient 3, as other two configurations give rise to regions of low TAWSS (Figure 6). In all CABG patient models with 2 mm SVG diameter, WSS_{avg} in the graft was more than 14 dynes/cm^2, and the local TAWSS was 20 – 60 dynes/cm^2 depending on the local diameter. These WSS are significantly higher than nominal WSS in SVGs in a range of 5 to 13 dynes/cm^3 reported in previous studies [16,17]. On the other hand, using SVG with 5 mm diameter leads to WSS_{avg} below 1.5 dynes/cm^2, lower than normal venous WSS of approximately 3 – 4 dynes/cm^2 [13]. Further, the interplay between vessel diameter and WSS, which has not been thoroughly reported in prior studies, could partly explain the conflicting conclusions on the superiority of sequential configuration in clinical studies. Focused analysis of clinical data is required to confirm this.

Regardless of the target coronary and revascularization geometry, the vein graft is subjected to elevated flows and pressures in the coronary circulation and the local TAWSS experienced by endothelial cells can be modulated by two factors – 1) the choice of the target

anastomosis [33], which governs flow through the graft and 2) the choice of diameter. Though subject to anatomic constraints, these choices are partially under a surgeon's control. In theory, a surgeon may be able to leverage our findings and methodology to control the TAWSS on the SVG, which may result in better surgical outcomes by selecting the optimal graft diameters and surgical configurations. To this end, pre-surgical patient specific modeling could be done to evaluate potential graft geometries. Physiologically, there seems to be a preferred setpoint in shear stress in the systemic arteries [34]. The existence of an optimal value of shear stress is unknown in a vein or a vein graft. However, as we identify optimal target values of TAWSS for improved patency, the modeling pipeline presented here provides a mechanism for patient-specific graft selection.

LIMITATIONS

As a result of the retrospective design of this study, the postoperative timepoint of the CT could not be controlled and the effects of vein remodeling post operation was not accounted for. Further, due to lack of measurements, the modulus values were assumed constant across patients discounting for variations with age and the associated remodeling. The number of patients simulated in this study is small and did not enable evaluation of all the possible Y and sequential configurations in a CABG. The model uses linear elastic assumption for vessel wall, not accounting for its nonlinear response or the deformation from the movement of the heart wall. We note that vein graft failure mechanisms are complex [30], and to date there is no single metric for identification of vein grafts susceptible to failure. Therefore, a multifactorial perspective should be incorporated in the analysis of expected graft patency. There is a further need to couple CFD simulations with models of vascular growth and remodeling and flow mediated dilatation to gain further insights into the pathophysiology of graft adaptation [11]. Our current efforts are geared towards sensitivity analysis and uncertainty quantification of CABG simulations taking into account inter- and intra- patient variabilities, discrepancies in blood pressure measurement, and use of literature data [26,35]. Future work will involve extending this framework to larger patient-cohorts and subsequently, validation against measurements and outcomes.

CONCLUSIONS

In this pilot study, we show that WSS varies with surgical anatomy and is patient-specific, that surgical geometry does not significantly affect coronary perfusion, and that graft diameter affects WSS, largely via inverse power scaling and Poiseuille derived WSS expression can be a useful guiding metric in these surgeries (Figure 7). WSS in the sequential graft is higher than Y and single grafts for a fixed diameter in the patient cohort. We exemplify how a virtual surgery paradigm can be used to guide clinical decision making in a non-invasive way, based on quantitative evaluations of hemodynamics. We envision that this framework may be useful in clinical practice to provide systematic comparisons of surgical options prior to surgery to improve graft patency and outcomes. The potential for virtual surgery to shift the paradigm in CABG surgery is promising.

Supplementary Material

Refer to Web version on PubMed Central for supplementary material.

ACKNOWLEDGEMENTS

We thank Mathew Irvin and Wendy Davilla for their assistance with IRB consent and clinical data collection. We acknowledge Christopher Chu and Christopher Jensen for their help with model building from CT data. We acknowledge Dr. Aekaansh Verma for his help with scripts to automate model building in SimVascular.

This work was supported by NIH grant (NIH R01-HL123698, NIH NIBIB R01-EB018302), NSF SSI grants 1663671 and 1339824, and NSF CDSE CBET 1508794. This work used the Extreme Science and Engineering Discovery Environment (XSEDE), which is supported by National Science Foundation grant number ACI-1548562. Patient recruitment and access to non-invasive clinical data was carried out according to protocols approved by the Stanford University and University of California San Diego Institutional Review Boards. Informed consent was obtained from all patients included in the study.

Glossary of abbreviations

CABG	Coronary artery bypass graft
SVG	Saphenous vein graft
TAWSS	Time averaged wall shear stress
OSI	Oscillatory Shear Index
CFD	Computational fluid dynamics
LAD	Left anterior descending artery
DIAG	Diagonal branch of left coronary artery
LCx	Left circumflex artery
OM	Obtuse marginal artery
RCA	Right coronary artery
PDA	Posterior descending artery
LIMA	Left internal mammary artery
RIMA	Right internal mammary artery

REFERENCES

1. van Brussel BL, et al. Different clinical outcome in coronary artery bypass with single and sequential vein grafts: A fifteen-year follow-up study. The Journal of Thoracic and Cardiovascular Surgery. 1996;112(1):69–78. [PubMed: 8691887]
2. Vural, ener, as demir O ong-term patency of sequential and individual saphenous vein coronary bypass grafts. European Journal of Cardio-thoracic Surgery. 2001;19:140–144. [PubMed: 11167102]
3. Park SJ, Kim HJ, Kim JB, Jung S-H, Choo SJ, Lee JW, et al. Sequential Versus Individual Saphenous Vein Grafting During Coronary Arterial Bypass Surgery. The Annals of Thoracic Surgery. 2020. In press.

4. Wallgren S, Nielsen S, Pan E, Pivodic A, Hansson EC, Malm CJ, et al. A single sequential snake saphenous vein graft versus separate left and right vein grafts in coronary artery bypass surgery: a population-based cohort study from the SWEDEHEART registry. European Journal of Cardio-Thoracic Surgery. 2019;56(3): 518–525. [PubMed: 30838388]
5. Goldman S, Zadina K, Krasnicka B, Moritz T, Sethi G, Copeland J et al. Predictors of Graft Patency 3 Years After Coronary Artery Bypass Graft Surgery. Journal of the American College of Cardiology. 1997;29(7):1563–1568. [PubMed: 9180120]
6. Mehta RH, Ferguson TB, Lopes RD, Hafley GE, Mack MJ, Kouchoukos NT et al. Saphenous Vein Grafts With Multiple Versus Single Distal Targets in Patients Undergoing Coronary Artery Bypass Surgery. Circulation. 2011;124:280–288. [PubMed: 21709060]
7. Yeh TJ, Heidary D, Shelton L. Y-Grafts and Sequential Grafts in Coronary Bypass Surgery: A Critical Evaluation of Patency Rates. The Annals of Thoracis Surgery. 1979;27(5):409–412.
8. Hulusi M, Basaran M, Ugurlucan M, Kocailik A, Basaran EK. Coronary artery bypass grafting with Y-saphenous vein grafts. Angiology. 2009;60:668–675. [PubMed: 19505884]
9. Shah PJ, Gordon I, Fuller J, Seevanayagam S, Rosalion A, Tatoulis J et al. Factors affecting saphenous vein graft patency: clinical and angiographic study in 1402 symptomatic patients operated on between 1977 and 1999. The Journal of Thoracic and Cardiovascular Surgery, 2003;126(6):1972–1977. [PubMed: 14688715]
10. Sarzaeem MR, Mandegar MH, Roshanali F, et al. Scoring system for predicting saphenous vein graft patency in coronary artery bypass grafting. Tex Heart Inst J. 2010;37(5):525–530. [PubMed: 20978562]
11. Ramachandra AB, Humphrey JD, Marsden AL. Gradual loading ameliorates maladaptation in computational simulations of vein graft growth and remodeling. J. R. Soc. Interface 2016; 14:20160995.
12. Ku DN, Giddens DP, Zarins CK, Glagov S. Pulsatile flow and atherosclerosis in the human carotid bifurcation. Positive correlation between plaque location and low oscillating shear stress. Arteriosclerosis, 1985;5(3):293–302. [PubMed: 3994585]
13. Gusic RJ, Myung R, Petko M, Gaynor JW, Gooch KJ. Shear stress and pressure modulate saphenous vein remodeling ex vivo. Journal of Biomechanics, 2005; 38(9):1760–1769. [PubMed: 16023463]
14. Jiang Z, Wu L, Miller BL, Goldman DR, Fernandez CM, Abouhamze ZS, et al. A novel vein graft model: adaptation to differential flow environments. American Journal of Physiology-Heart and Circulatory Physiology, 2004; 286(1):H240–H245. [PubMed: 14500133]
15. Sankaran S, Moghadam ME, Kahn AM, Tseng EE, Guccione JM, Marsden AL. Patient-specific multiscale modeling of blood flow for coronary artery bypass graft surgery. Annals of Biomedical Engineering. 2012;40:2228–2242. [PubMed: 22539149]
16. Ramachandra AB, Kahn AM, Marsden AL. Patient-specific simulations reveal significant differences in mechanical stimuli in venous and arterial coronary grafts. Journal of Cardiovascular Translational Research. 2016;9:279–290. [PubMed: 27447176]
17. Khan MO, Tran JS, Han Z, Boyd J, Packard RRS, Karlsberg RP, et al. Low Wall Shear Stress is Associated with Saphenous Vein Graft Stenosis in Patients with Coronary Artery Bypass Grafting. Journal of Cardiovascular Translational Research. 2020.
18. Ballarin F, Faggiano E, Manzoni A, et al. Numerical modeling of hemodynamics scenarios of patient-specific coronary artery bypass grafts. Biomechanics and Modeling in Mechanobiology. 2017;16:1373–1399. [PubMed: 28289915]
19. Mao B, Zhao Z, Li B, Feng Y, Feng Y, Liu Y, The comparisons of venous sequential, normal graft patency based on hemodynamics, Journal of Mechanics in Medicine and Biology, 2020;20(02):1950080.
20. Updegrove A, Wilson NM, Merkow J, Lan H, Marsden AL, Shadden SC. Simvascular: An open source pipeline for cardiovascular simulation. Annals of Biomedical Engineering. 2017;45:525–541. [PubMed: 27933407]
21. Kim HJ, Vignon Clementel I, Figueroa C, La Disa J, Jansen K, Feinstein F, et al. On coupling a lumped parameter heart model and a three-dimensional finite element aorta model. Annals of Biomedical Engineering, 2009;37(11):2153–2169. [PubMed: 19609676]

22. Figueroa CA, Vignon-Clementel IE, Jansen KE, Hughes TJ, Taylor CA. A coupled momentum method for modeling blood flow in three-dimensional deformable arteries. Computer Methods in Applied Mechanics and Engineering. 2006;195:5685–5706.
23. Podesser BK, Neumann F, Neumann M, Schreiner W, Wollenek G, Mallinger R. Outer radius-wall thickness ratio, a postmortem quantitative histology in human coronary arteries. Acta Anat (Basel). 1998;163(2):63–68. doi:10.1159/000046485 [PubMed: 9873135]
24. O' Neill MJ, Wolf PD, O' Neill TK, Montesano RM, Waldhausen JA. A rationale for the use of sequential coronary artery bypass grafts. Journal of Thoracic and Cardiovascular Surgery.1981;81:686–690. [PubMed: 6971376]
25. Une D, Kulik A, Voisine P, Le May M, Ruel M. Correlates of Saphenous Vein Graft Hyperplasia and Occlusion 1 Year After Coronary Artery Bypass Grafting. Circulation. 2013;128(No.11_suppl_1):S213–S218. [PubMed: 24030409]
26. Seo J, Schiavazzi DE, Kahn AM, Marsden AL. The effects of clinically-derived parametric data uncertainty in patient-specific coronary simulations with deformable walls. International Journal for Numerical Methods in Biomedical Engineering. 2020;e3351. [PubMed: 32419369]
27. Zamir M. The role of shear forces in arterial branching. The Journal of General Physiology, 1976;67:213–222. [PubMed: 1255127]
28. Li J, Gu C. Comparison of blood flow in single and sequential vein grafts during off-pump coronary artery bypass. Journal of Thoracic Disease. 2019;11(8):3341–3346. [PubMed: 31559037]
29. Murray CD. The Physiological Principle of Minimum Work: I. The Vascular System andthe Cost of Blood Volume. Proc Natl Acad Sci USA. 1926;12(3):207–214. [PubMed: 16576980]
30. de Vries MR, Simons KH, Jukema JW, Braun J, Quax PHA. Vein graft failure: from pathophysiology to clinical outcomes. Nature Reviews Cardiology. 2016;13:451–470. [PubMed: 27194091]
31. Hwang HY, Koo B-K, Yeom SY, Kim TK, Kim K-B. Endothelial Shear Stress of the Saphenous Vein Composite Graft Based on the Internal Thoracic Artery, The Annals of Thoracic Surgery. 2018;105(2):P564–571.
32. Fry DL. Certain histological and chemical responses of the vascular interface to acutely induced mechanical stress in the aorta of the dog. Circulation research 24.1 (1969): 93–108. [PubMed: 5763742]
33. Roth JA, Cukingnan RA, Brown BG, Gocka E, Carey JS. Factors Influencing Patency of Saphenous Vein Grafts. The Annals of Thoracic Surgery. 1978;28(2):176–183
34. Lehoux S. Molecular mechanisms of the vascular responses to hemodynamic forces. Biomechanics of Coronary Atherosclerotic Plaque. Academic Press, 2020. 51–88.
35. Tran JS, Schiavazzai DE, Kahn AM, Masrden AL. Uncertainty quantification of simulated biomechanical stimuli in coronary artery bypass grafts. Computer Methods in Applied Mechanics and Engineering. 2020, 345, 402–428.

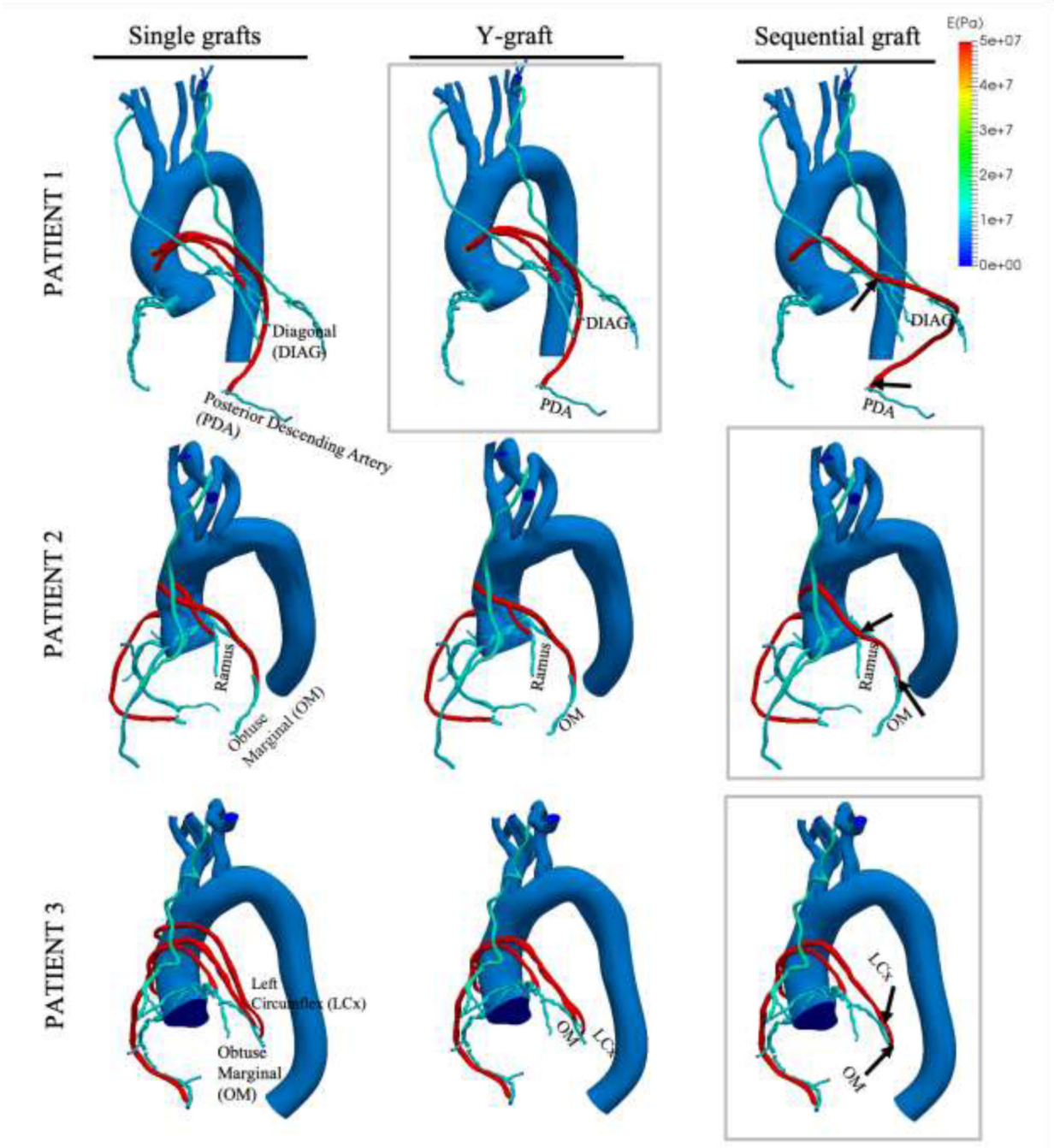

Figure 1:

Patient-specific models from CT scan of three patients who had undergone CABG surgery with the corresponding virtual modification on venous grafts to single, Y, and sequential configurations. Vessels are colored by their modulus values, E (Pa). DIAG – diagonal branch of left coronary artery, PDA – posterior descending artery, OM – obtuse marginal, LCx – left circumflex artery. Arrows indicate the proximal and distal anastomoses in the sequential graft. Baseline clinical geometry is marked by the gray box.

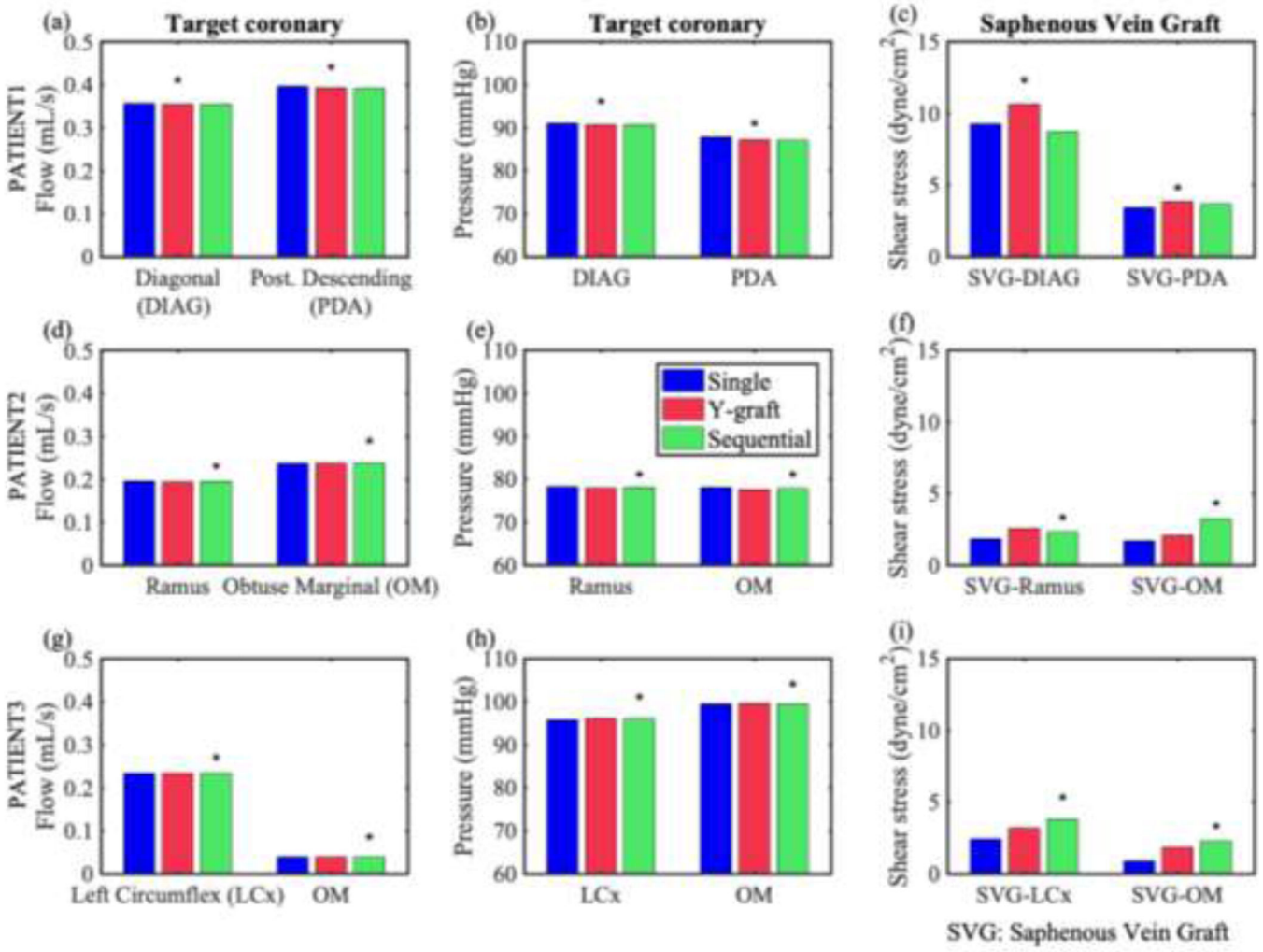

Figure 2:

Summary of mean flow rates (a,d,g) and pressures (b,e,h) at target coronary arteries connected to SVG, and time and spatially averaged wall shear stress ($WSS_{avg,}$ (c,f,i)) on the vein graft with different configurations. Notice that the flow to the distal coronary and pressure in the graft is independent of the choice of revascularization geometry. The wall shear stress is variable across patients and surgical geometries, however. DIAG – diagonal branch of left coronary artery, PDA – posterior descending artery, OM – obtuse marginal, LCx – left circumflex artery. Baseline clinical geometry is marked by the gray box.

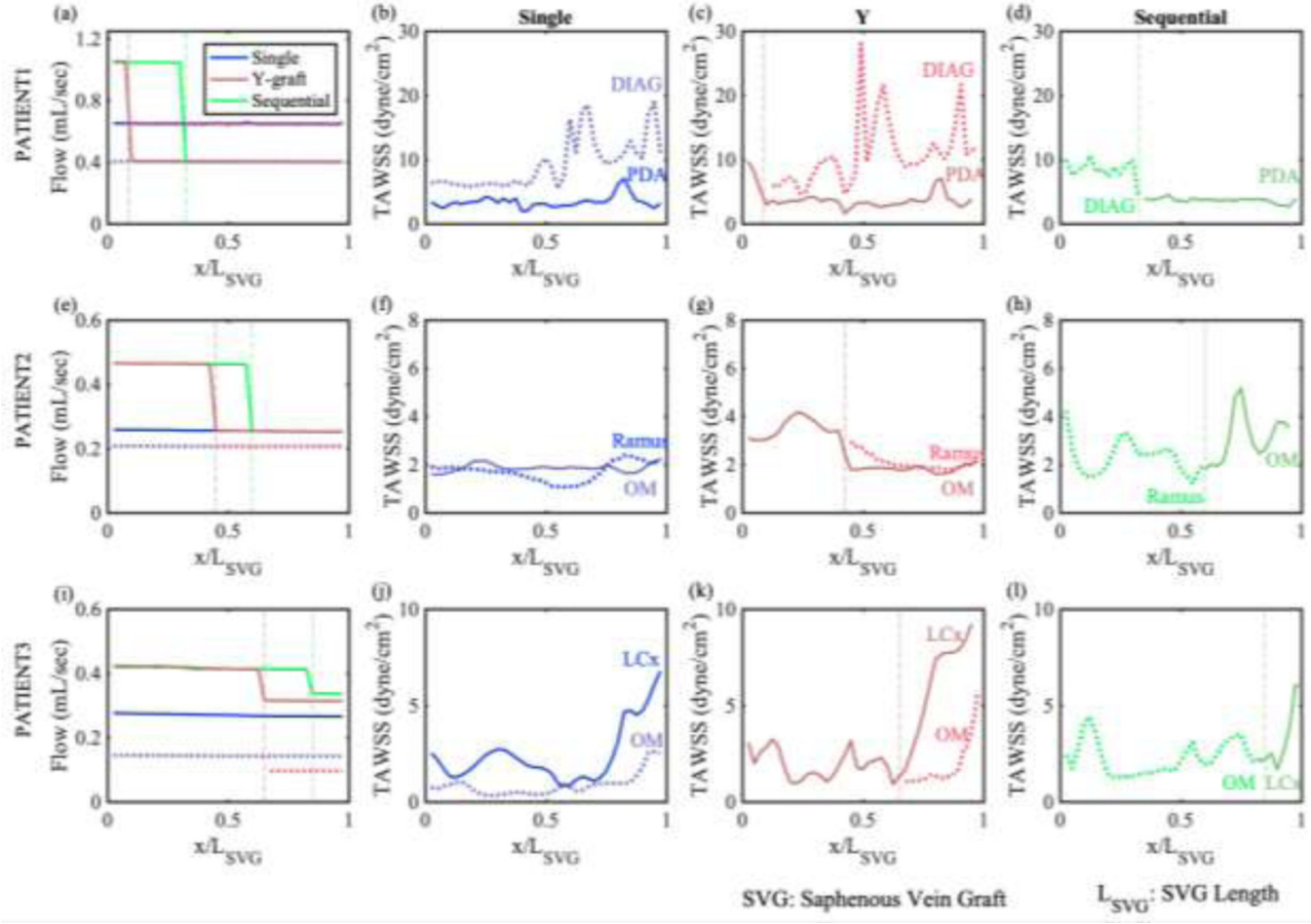

Figure 3:

Flow rates and time-averaged wall shear stress (TAWSS) distributions along the centerline of vein grafts in each patient. x is the location along the centerline, and L_{SVG} is the length of the respective graft. Solid and dotted lines are the cross-section averaged TAWSS and dashed-dotted lines are the location of first anastomosis in the sequential graft (green), or bifurcation in the y-graft (red). In (a), (e), (i), the solid lines and the dotted lines are plotted to show the flow rates in the two branches in the single and Y-graft, while the solid lines in the Y-graft include the trunk. Flow rate is constant along the length of the graft until it reaches an anastomotic point, due to mass conservation. The TAWSS is highly variable along the length of the graft, due to diameter variations.

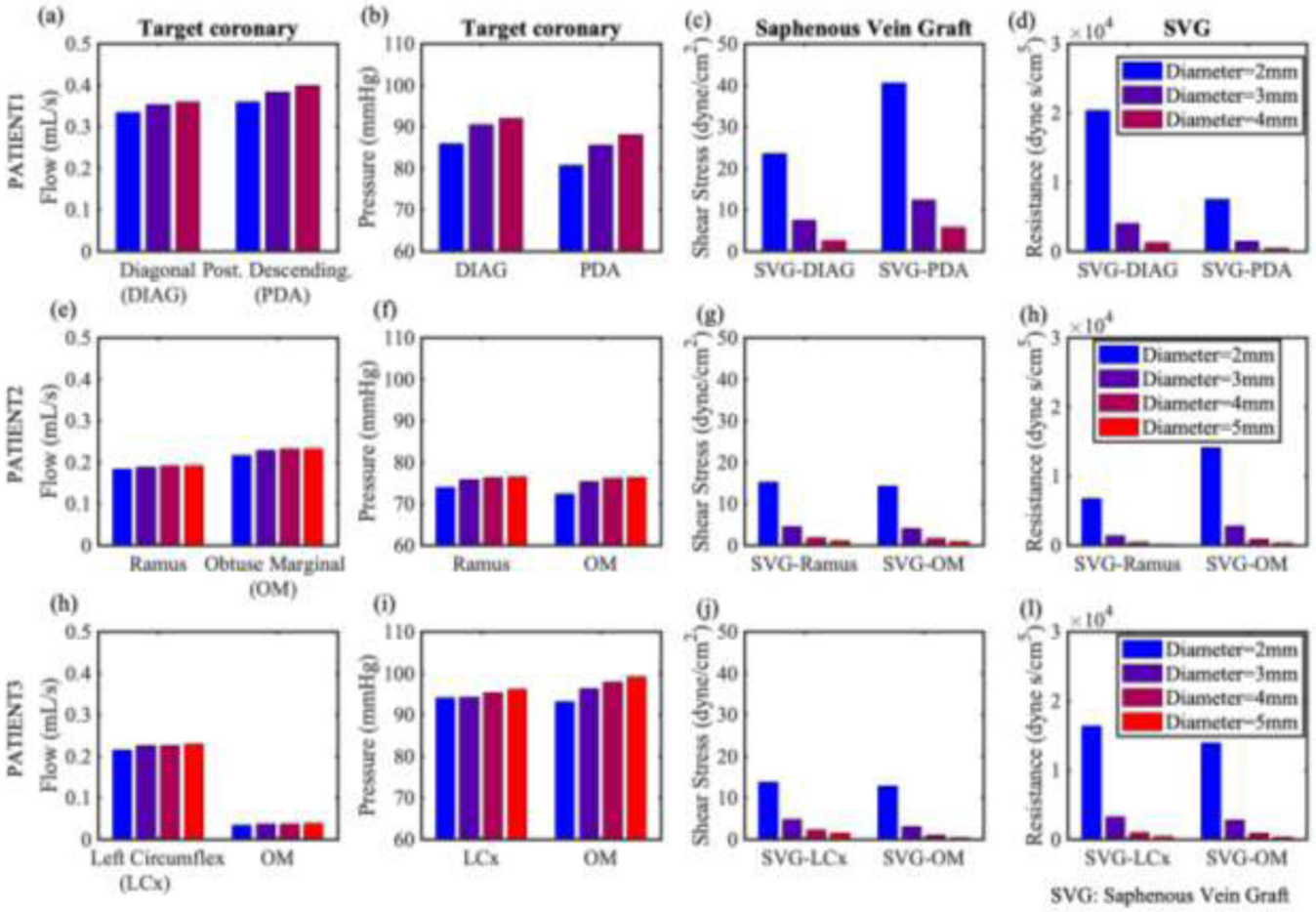

Figure 4:

Summary of mean flow rate (a,e,h) and pressure (b,f,i) at target coronary arteries connected to single saphenous vein grafts (SVG), time and spatially averaged wall shear stress (WSS_{avg}) (c,g,j), vascular resistance of the vein graft with varying diameter from 2 mm to 5 mm (d,h,l) from 3D CFD simulations. DIAG – diagonal branch of the left coronary artery, PDA – posterior descending artery, OM – obtuse marginal, LCx – left circumflex artery.

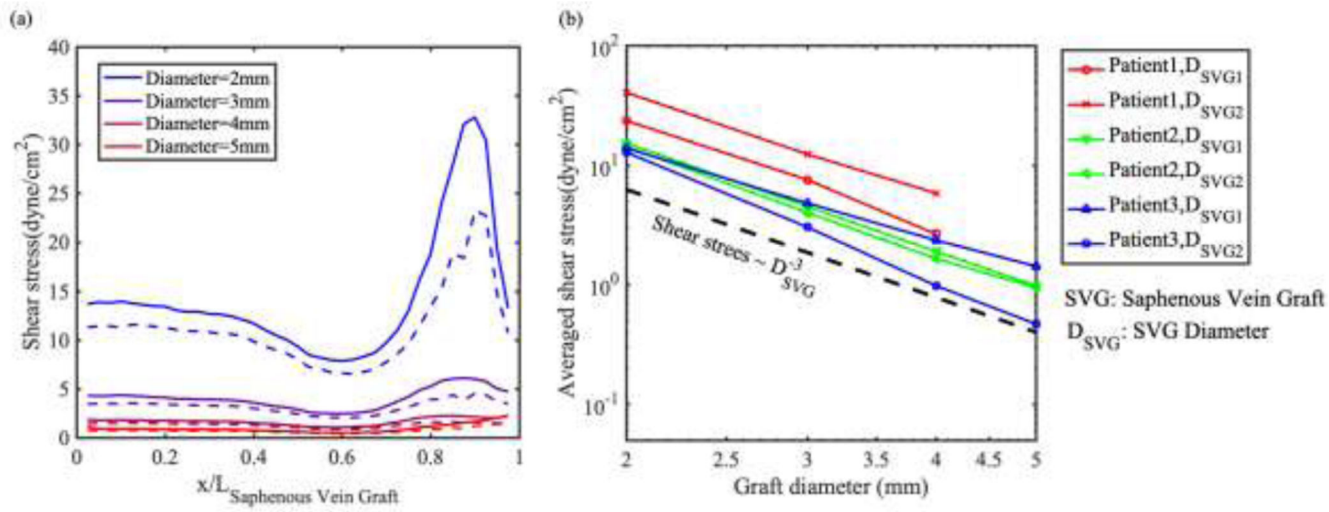

Figure 5:

Time-averaged wall shear stress distributions along the centerline of a vein graft in SVG connected to OM in Patient 2. x is the location along the centerline, and L_{SVG} is the length of the saphenous vein graft. Solid lines are data from 3-D CFD simulation, and dashed lines are estimated from Poiseuille flow relationship. (b) The scaling of WSS_{avg} on the grafts to the diameter, D_{SVG}. The dashed line is $WSS_{avg} \sim D_{SVG}{}^{-3}$.

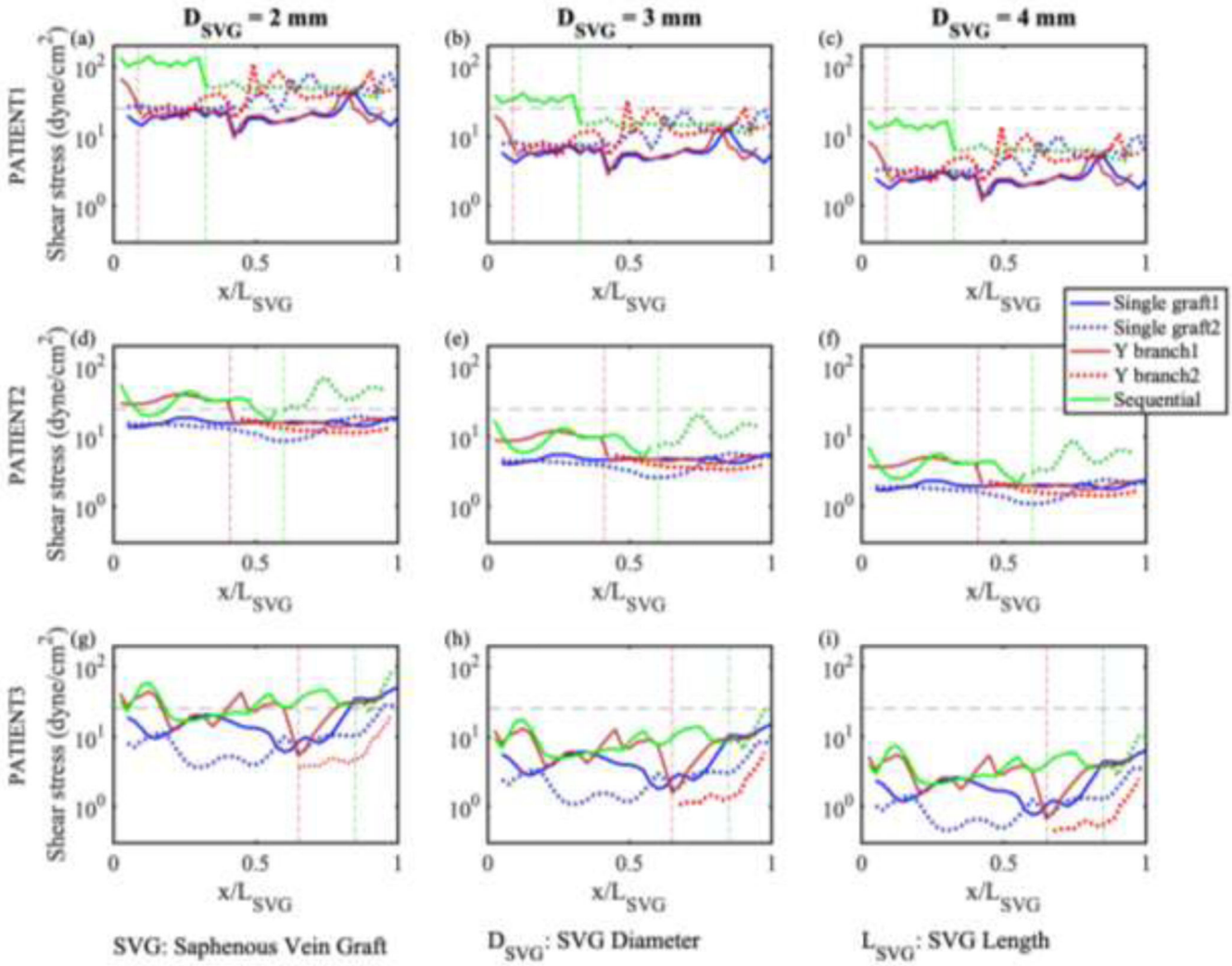

Figure 6:

Virtually evaluated time-averaged wall shear stress (TAWSS) vein grafts in each patient with D_{SVG} = 2 mm (a,d,g), D_{SVG} = 3 mm (b,e,h), D_{SVG} = 4 mm (c,f,i) computed with Poiseuille assumptions. The TAWSS in Figure 4 is rescaled by the factor of $D^3_{SVG}/D^3_{SVG\text{-}Original}$. x is the location along the centerline, and L_{SVG} is the length of each graft. Solid and dotted lines are the extrapolated TAWSS and dashed-dotted lines are the location of first anastomosis in the sequential graft (green), or bifurcation in the y-graft (red). The dashed lines are 25 dynes/cm^2. Note that the TAWSS can be modulated to reach physiological, or pathologically low or high values by only changing the diameter of the graft.

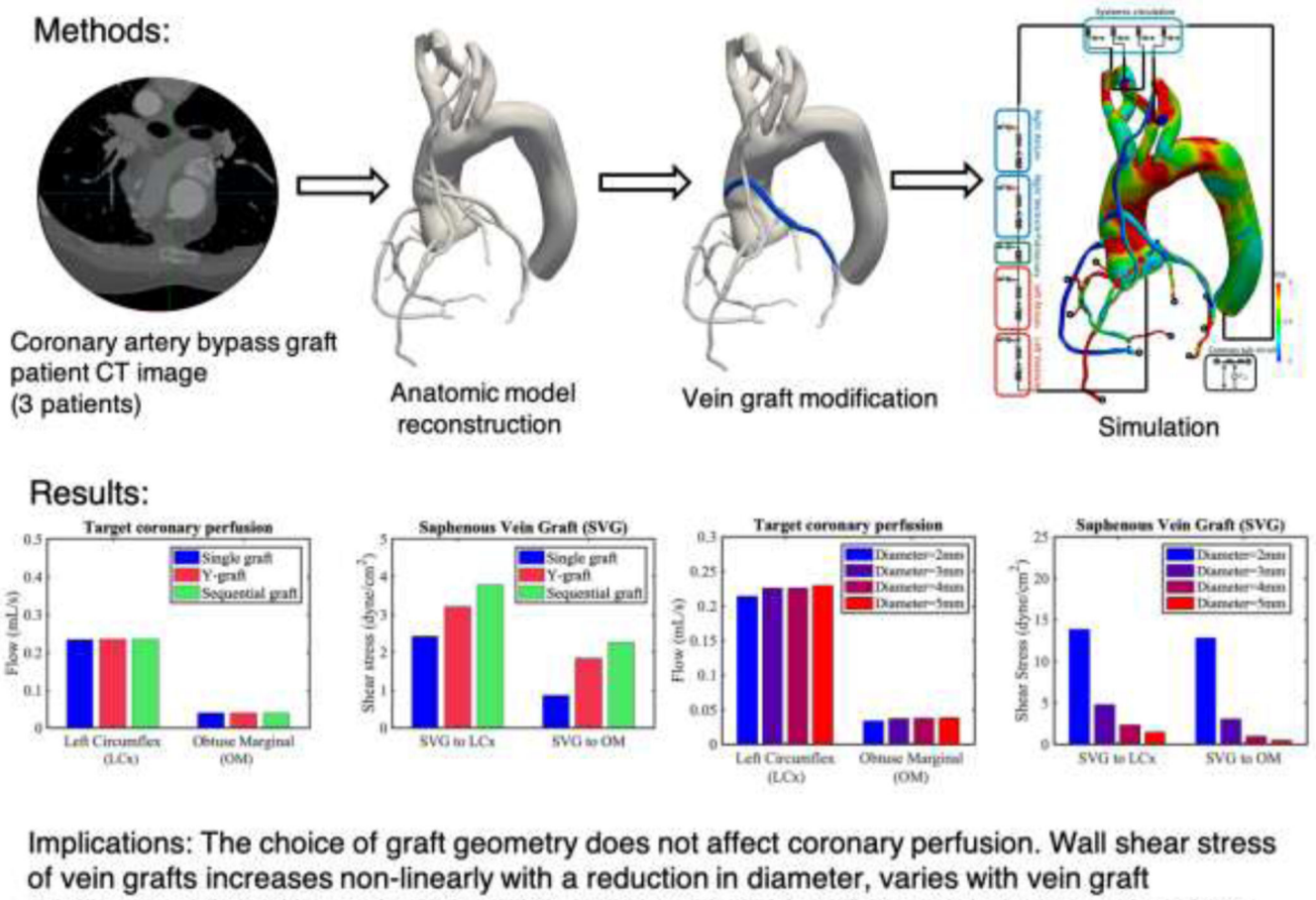

Figure 7.

Graphical summary of workflow and representative results for one patient. Cardiac CT data are used to construct a three-dimensional anatomic model of aorta, coronary arteries and bypass grafts. Modifications to the vein graft geometry are made. Computational fluid dynamic simulation are performed using the resultant model coupled with lumped parameter zero-dimensional circuit models of cardiac, coronary, and systemic circulations to compute vessel flow rates and wall shear stress for different geometries.

Table 1:

Summary of patient demographics, the grafts configurations, geometric characteristics of SVGs, and vascular resistance of SVGs and target coronaries. Prox. – proximal target coronary. Dist. – distal target coronary, SVG – saphenous vein graft, RIMA – right internal mammary artery, LIMA – left internal mammary artery, DIAG- diagonal branch, OM – obtuse marginal artery, PDA – posterior descending artery, LAD – left anterior descending, RCA – right coronary artery, LCx – left circumflex artery, RU – Resistance unit, 10^3 dyne · s/cm. The length of Y-graft SVG to the distal target coronaries include the trunk.

Patient ID		**Patient 1**		**Patient 2**		**Patient 3**	
Gender		Male		Male		Male	
Age (years)		60		55		77	
Interval after CABG		1 month		14 years		14 years	
Grafts in patients (Target coronaries)		Y-SVG graft (DIAG, PDA) RIMA (LAD) LIMA (OM)		Sequential SVG (Ramus, OM) SVG (RCA)LIMA (LAD)		Sequential SVG(OM, LCx)SVG (Ramus)SVG (PDA)LIMA (LAD)	
Target coronaries of virtually modified SVGs		DIAG (Prox.)	PDA (Dist.)	Ramus (Prox.)	OM (Dist.)	OM (Prox.)	LCx (Dist.)
Single SVG	Diameter (mm)	3.1	3.6	4.0	4.1	4.4	3.9
	Length (cm)	7.4	20.0	6.6	13.8	13.7	16.1
	Resistance (RU)	1.3	1.9	0.4	0.8	0.9	1.0
Y-graft SVG	Diameter (mm)	3.6	3.1	3.7	4.1	2.8	3.9
	Length (cm)	5.9	20.7	2.7	14.0	16.2	2.5
	Resistance (RU)	1.4		0.6		1.1	
Sequential SVG	Diameter (mm)	3.6		4.3		4.4	
	Length (cm)	25.6		13.6		15.5	
	Resistance (RU)	2.6		0.7		0.7	
Coronary Resistance (RU)		323.2	279.9	416.6	345.2	2887.6	352.9